

Supersonic Jet Studies of Alkyl-Substituted Pyrazines and Pyridines. Minimum Energy Conformations and Torsional Motion

Jeffrey I. Seeman,^{*,†} John B. Paine, III,[†] Henry V. Secor,[†] Hoong-Sun Im,[‡] and E. R. Bernstein^{*,‡}

Contribution from the Philip Morris Research Center, P.O. Box 26583, Richmond, Virginia 23261, and the Department of Chemistry, Colorado State University, Fort Collins, Colorado 80523. Received December 5, 1990.
Revised Manuscript Received April 11, 1991

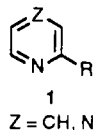
Abstract: Conformational preferences for methyl-, ethyl-, propyl-, and isopropyl-substituted pyrazines and pyridines are determined by mass resolved excitation spectroscopy (MRES) and MOPAC 5/PM3 semiempirical calculations. The results of these studies suggest that the conformational behavior of alkyl-substituted pyrazines and pyridines is different from that of alkyl-substituted benzenes. Based on the experimental and semiempirical theoretical results reported herein and published ab initio calculations, this difference can be attributed to a stabilizing interaction between an α -hydrogen atom of the alkyl substituent and the adjacent lone pair nonbonding electrons on the ring nitrogen atom.

I. Introduction

The azines, or azabenzene, are a valuable and fascinating series of compounds which are related to benzene through the substitution of one or more C-H fragments by nitrogen atoms. Azines form the basic structures of innumerable alkaloids and of numerous molecules of both practical and theoretical interest.¹ Various naturally occurring and synthetic pyridines, pyrazines, and related compounds are known to possess unique and intense flavors and fragrances.^{1c} A continuing, fascinating area of both basic research and practical application is an understanding of the relationship between structure and biological properties for the simple azines. Consequently, studies of the structural and electronic characteristics of azines have great significance.

Many investigations have been reported on σ - and π -electron distributions of azines, on their altered chemical reactivity compared with analogous benzenes, and on their resonance energies.² In contrast, the conformational analysis of substituted azines has received scant attention. This is unfortunate, given the effect that conformation has on physical, chemical, and biological properties and processes. A similar situation existed for saturated alicyclic hydrocarbons versus saturated heterocycles; thus conformational analysis for cyclohexanes^{3a} had a history of over 20 years prior to the emergence of similar systematic studies of, for example, piperidines.^{3b}

Perhaps most interesting of the substituted azines are those compounds bearing substituents α to the nitrogen atom, e.g., 1.

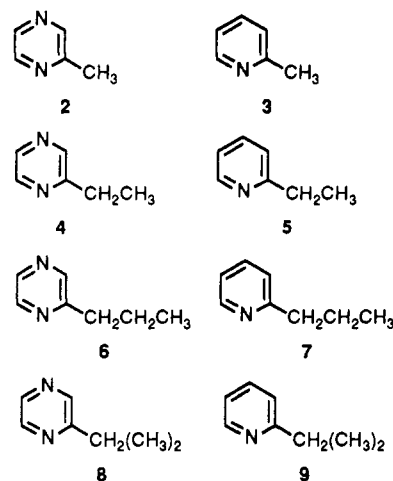


R = alkyl, halogen, oxygen, heteroalkyl, etc.

Indeed, most of the structural information to date on compounds such as 1 comes from direct comparison with and extrapolation from data on related benzenes.⁴ Because empirical force fields for heterocycles have not been available until recently,^{5,6} almost all the theoretical studies to date have been done using semiempirical methods.^{7,8}

In this paper, we report the application of mass resolved excitation spectroscopy (MRES, sometimes referred to as time-of-flight mass spectroscopy^{9,10}) to the conformational analysis of α -alkyl-substituted pyridines and pyrazines. Recently, MRES has been utilized to identify the minimum energy conformations

Chart I



of various alkyl- and hetero-substituted benzenes in the gas phase. Included in the list of substituents studied thus far are methyl,^{9a,b}

(1) (a) *The Alkaloids, Chemistry and Pharmacology*; Brossi, A., Ed.; Academic Press: San Diego, CA, 1989, Vol. 36 and other volumes in this series. (b) *Comprehensive Heterocyclic Chemistry*; Pergamon Press: Oxford, UK, 1985. (c) Seeman, J. I.; Ennis, D. M.; Secor, H. V.; Clawson, L.; Palen, J. *Chem. Senses* 1989, 14, 395 and references cited therein.

(2) For leading references, see: (a) Wiberg, K. B.; Nakaji, D.; Breneman, C. M. *J. Am. Chem. Soc.* 1989, 111, 4178. (b) Katritzky, A. R. *Handbook of Heterocyclic Chemistry*; Pergamon Press: New York, 1985.

(3) For historical perspectives and leading references, see: (a) Barton, D. H. R. Some Recollections of Gap Jumping. In *Profiles, Pathways, and Dreams*; Seeman, J. I., Ed.; American Chemical Society: Washington, DC, 1991. (b) Eliel, E. L. From Cologne to Chapel Hill. In *Profiles, Pathways, and Dreams*; Seeman, J. I., Ed.; American Chemical Society: Washington, DC, 1990.

(4) (a) Öki, M. *Applications of Dynamic NMR Spectroscopy to Organic Chemistry*; VCH Publishers: Deerfield Beach, FL, 1985. (b) Jackman, L. M.; Cotton, F. A., Eds. *Dynamic NMR Spectroscopy*; Academic Press: New York, 1975. (c) Berg, U.; Liljefors, T.; Roussel, C.; Sandström, J. *Acc. Chem. Res.* 1985, 18, 80. (d) Berg, U.; Sandström, J. *Adv. Phys. Org. Chem.* 1989, 25, 1. (e) Kao, J. *J. Am. Chem. Soc.* 1987, 109, 3817. (f) Seeman, J. I. *Pure Appl. Chem.* 1987, 59, 1661.

(5) Kao, J. *J. Comput. Chem.* 1988, 9, 905.

(6) Berg, U.; Gallo, R. *Acta Chem. Scand.* 1983, B37, 661.

(7) Warshel, A.; Lippicirella, A. *J. Am. Chem. Soc.* 1981, 103, 4664.

(8) For examples from our work, see: (a) Seeman, J. I.; Schug, J. C.; Viers, J. C. *J. Org. Chem.* 1983, 48, 2399. (b) Schug, J. C.; Viers, J. C.; Seeman, J. I. *J. Org. Chem.* 1983, 48, 4892. (c) Seeman, J. I.; Viers, J. W.; Schug, J. C.; Stovall, M. D. *J. Am. Chem. Soc.* 1984, 106, 143.

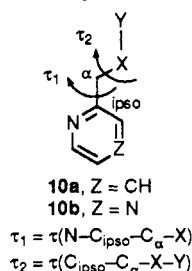
* To whom correspondence should be addressed.

† Philip Morris Research Center.

‡ Colorado State University.

ethyl,^{9a,c,d} propyl^{9a,d,11} and isopropyl,^{9e} *tert*-butyl,^{9e} vinyl,^{9f,10a} allyl,^{9g} methoxy,^{9h} ethoxy,⁹ⁱ hydroxymethyl,^{9j} aminomethyl,^{9k} hydroxy,^{10b-d} and carbomethoxy.^{10e} The work described herein represents one of the few experimental conformational analysis studies of substituted nitrogen heteroaromatic compounds and the first such study of alkyl-substituted heterocyclic systems employing MRES.^{12,13}

This investigation has two goals: (1) the determination of the minimum energy conformation(s) of methyl-, ethyl-, propyl-, and isopropyl-substituted pyrazines and pyridines (2-9; see Chart I), as defined by the torsional angles τ_1 and τ_2 as shown in 10; and



(2) the examination of the torsional motion of these substituents. At the initiation of this project, we were not certain that substituted pyridines and pyrazines would possess the requisite photophysical properties (i.e., relative geometries, lifetimes, quantum yields, etc.) necessary for the successful observation of spectra. In fact, the nonradiative (internal conversion and intersystem crossing) rates for many 3- and 4-substituted pyridines are too fast to allow fluorescence excitation or MRES to be obtained.¹⁴

Mass resolved excitation spectra (MRES) of the $S_1 \leftarrow S_0$ transition of 2-9 and a number of deuterated and polysubstituted derivatives are reported herein. In conjunction with these experimental efforts, we employ MOPAC 5/PM3 calculations to provide additional information on the conformational properties

(9) (a) Breen, P. J.; Warren, J. A.; Bernstein, E. R.; Seeman, J. I. *J. Am. Chem. Soc.* **1987**, *109*, 3453. (b) Breen, P. J.; Warren, J. A.; Bernstein, E. R.; Seeman, J. I. *J. Chem. Phys.* **1987**, *87*, 1917. (c) Breen, P. J.; Bernstein, E. R.; Seeman, J. I. *J. Chem. Phys.* **1987**, *87*, 3269. (d) Breen, P. J.; Warren, J. A.; Bernstein, E. R.; Seeman, J. I. *J. Chem. Phys.* **1987**, *87*, 1927. (e) Seeman, J. I.; Secor, H. V.; Breen, P. J.; Grassian, V. H.; Bernstein, E. R. *J. Am. Chem. Soc.* **1989**, *111*, 3140. (f) Grassian, V. H.; Bernstein, E. R.; Secor, H. V.; Seeman, J. I. *J. Phys. Chem.* **1989**, *93*, 3470. (g) Breen, P. J.; Bernstein, E. R.; Secor, H. V.; Seeman, J. I. *J. Phys. Chem.* **1989**, *93*, 6731. (h) Breen, P. J.; Bernstein, E. R.; Secor, H. V.; Seeman, J. I. *J. Am. Chem. Soc.* **1989**, *111*, 1958. (i) Bernstein, E. R.; Im, H.-S.; Young, M. A.; Secor, H. V.; Bassfield, R. L.; Seeman, J. I. *J. Org. Chem.* **1991**, *56*, 6059. (j) Seeman, J. I.; Secor, H. V.; Im, H.-S.; Bernstein, E. R. *J. Chem. Soc., Chem. Commun.* **1990**, 87. (k) Im, H.-S.; Bernstein, E. R.; Secor, H. V.; Seeman, J. I. *J. Am. Chem. Soc.* **1991**, *113*, 4422. (l) Li, S.; Bernstein, E. R.; Secor, H. V.; Seeman, J. I. *Tetrahedron Lett.* **1991**, 3945.

(10) (a) Hollas, J. M.; Bin Husein, M. Z. *Chem. Phys. Lett.* **1989**, *154*, 228. (b) Oikawa, A.; Abe, H.; Mikami, N.; Ito, M. *J. Phys. Chem.* **1984**, *88*, 5180. (c) Okuyama, K.; Mikami, N.; Ito, M. *J. Phys. Chem.* **1985**, *89*, 5617. (d) Mizuno, H.; Okuyama, K.; Ebata, T.; Ito, M. *J. Phys. Chem.* **1987**, *91*, 5589. (e) Howells, B. D.; Martinez, M. T.; Palmer, T. F.; Simons, J. P.; Walters, A. *J. Chem. Soc., Faraday Trans.* **1990**, *86*, 1949.

(11) Song, X.; Pauls, S.; Lucia, J.; Du, P.; Davidson, E. R.; Reilly, J. P. *J. Am. Chem. Soc.* **1991**, *113*, 3202.

(12) For a discussion on the power dependence technique for assigning origins, and applications to tryptophan and tryptophan derivatives, see: (a) Rizzo, T. R.; Park, Y. D.; Peteanu, L. A.; Levy, D. H. *J. Chem. Phys.* **1986**, *84*, 2534. For more recent papers on this subject, see: (b) Tubergen, M. J.; Cable, J. R.; Levy, D. H. *J. Chem. Phys.* **1990**, *92*, 51. (c) Tubergen, M. J.; Levy, D. H. *J. Phys. Chem.* **1991**, *95*, 2175. (d) Teh, C. K.; Sipior, J.; Sulkes, M. *J. Phys. Chem.* **1989**, *93*, 5393 and other papers in this series.

(13) (a) Tomer, J. L.; Yamauchi, S.; Pratt, D. W. *Chem. Phys. Lett.* **1990**, *175*, 30. We thank Professor Pratt for making available a copy of his manuscript prior to publication and for helpful discussions. (b) Methyl groups attached to heterocyclic rings but not α to a nitrogen appear to have a rotational barrier similar to that of the methyl group in toluene. Thus, a small methyl rotational barrier has been found for 4-picoline, by experiment^{13c} (13.7 cal/mol) and by theory (14 cal/mol by ab initio methods).^{13c} (c) Zweers, A. E.; Brom, H. B.; Huiskamp, W. *J. Phys. Lett. A* **1974**, *47*, 347. (d) Moffat, J. B. *J. Mol. Struct.* **1976**, *32*, 67. (e) Arenas, J. F.; Lopez-Navarrete, J. T.; Marcos, J. I.; Otero, J. C. *J. Mol. Struct.* **1986**, *142*, 423. (f) Arenas, J. F.; Lopez-Navarrete, J. T.; Marcos, J. I.; Otero, J. C. *J. Mol. Struct.* **1987**, *162*, 263. (g) Arenas, J. F.; Hernandez, V.; Marcos, J. I.; Otero, J. C. *J. Mol. Struct.* **1988**, *189*, 307.

(14) Bernstein, E. R.; Breen, P. J.; Im, H.-S. Unpublished results.

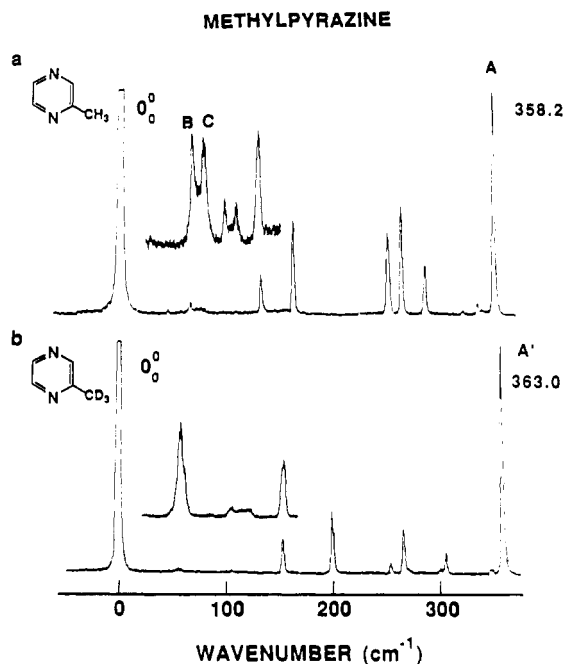


Figure 1. MRES of jet cooled (a) methylpyrazine (2) and (b) methyl- d_3 -pyrazine (11) around their 0_0^0 transition regions. Intense origins at 30945.3 and 30937.7 cm^{-1} are found for 2 and 11, respectively. The next strong peaks at 358.2 and 363.0 cm^{-1} for 2 and 11 (A and A', respectively) are assigned as ν_{13} . The spectra shown as inserts are taken with low backing pressures (see Figures 2 and 3).

of some of these molecules. The logic, techniques, and methods for the conformational analysis have been previously outlined in some detail.^{9,15} By using suitably substituted molecules, one can assign the geometry of the stable conformation(s) of a molecule by comparing the number of stable conformations observed with the number of stable conformations predicted for specific "hypothetical energy minima". The MRES technique provides a means to count the number of stable conformations in a manner analogous to that obtained using dynamic NMR experiments.

The MRES experiment is performed in the following manner. A sample is irradiated with a laser of energy ν_1 , resulting in the generation of the first excited singlet state ($S_1 \leftarrow S_0$). A second photon ν_2 subsequently ionizes those molecules in S_1 ($I \leftarrow S_1$). The ions are detected in given mass channels by time-of-flight mass spectroscopy, such that only ion current representing a chosen m/z is recorded. The energy of the ν_1 laser is scanned, and an $S_1 \leftarrow S_0$ excitation spectrum of a mass selected species is obtained.

The unique qualities of the MRES technique, based on previous experimental results,^{9,15} are summarized as follows: (1) conformational interconversions of a molecule are halted by the rapid cooling which occurs in a supersonic expansion (within 1-2 mm of the expansion nozzle, the effective internal temperature of the molecules is ca. 10 K); (2) the optical absorption process occurs much more rapidly than nuclear motion; (3) each different conformation of a molecule has its own spectroscopic properties which can be accessed and distinguished through optical ($S_1 \leftarrow S_0$) excitation; and (4) the features around the origin (0_0^0 transition) of the $S_1 \leftarrow S_0$ excitation can be analyzed to yield the number of stable conformations of the species under study.

The observation of a single origin transition in this work implies that either (a) only a single stable ground state conformation exists, (b) one conformation is significantly more stable than the others, or less likely, but possible, (c) the transition energies for two origin transitions are unresolved. Observation of a number of transitions in the 0_0^0 region is a complicating result which requires the distinction between actual origin transitions and low energy vibronic transitions. One strategy which we have used successfully in the past⁹ has been to obtain MRES of specifically deuterated derivatives of the substrate of interest. In general, the origin

(15) Bernstein, E. R.; Law, K.; Schauer, M. *J. Chem. Phys.* **1984**, *80*, 207.

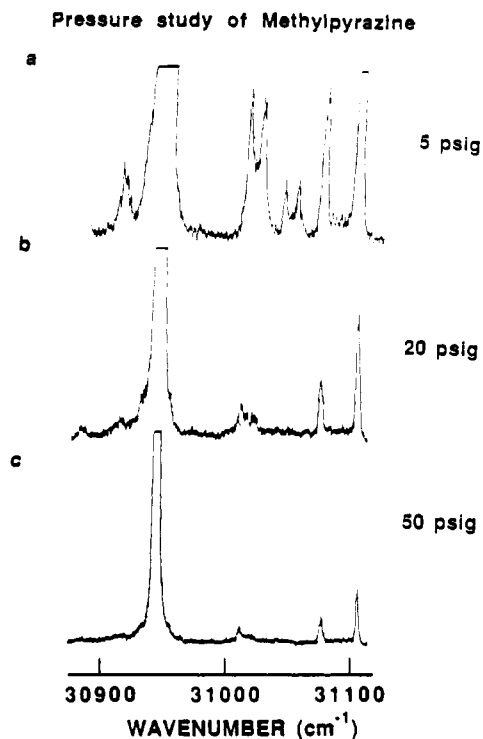


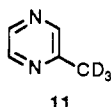
Figure 2. Expansion pressure study of methylpyrazine (**2**). The backing pressures applied are indicated. The two doublets near the origin show characteristic hot band behavior.

transitions of the various conformers undergo little or no relative shift upon deuteration of the compounds studied, while the various vibronic transitions do evidence much more substantial relative shifts. This difference in behavior of conformer origin transitions and vibronic transitions with respect to deuteration of the substrate arises because the zero point energy of the molecule in the two electronic states involved in the transition is the average of the (positive and negative) individual vibration isotope shifts in each state. These contributions to the isotopic zero point energy of the conformers tend to average to zero in each state as well as between states. The individual vibrational isotope shifts are built upon these averages and can, of course, be much larger. By comparing the MRES of a compound with the MRES of its deuterated derivative, conformer origin transitions can frequently be assigned as the features in the spectrum that do not shift under isotopic substitution of the substrate.¹²

As described above, the deuterated derivatives are used in the MRES experiments to distinguish between origin transitions, which do not show isotope shifts, and vibrational transitions, which do show isotope shifts, relative to the MRES of the parent compound.

II. Results and Discussion

A. Methylpyrazine (2), 2-Methylpyridine (3), and Related Compounds. The MRES of methylpyrazine (**2**) and methyl-*d*₃-pyrazine (**11**) are displayed in Figure 1, a and b, respectively. The origin of the $S_1 \leftarrow S_0$ transition of **2** occurs at 30945.3 cm⁻¹. Peak A at 358.2 cm⁻¹ to higher energy of the origin is assigned as ν_{10a} .¹⁶ Between these two peaks (the origin and ν_{10a}), several weak features appear in the absorption spectrum. The MRES of **11** contains a single origin at 30937.7 cm⁻¹ and one strong



feature (peak A') at 363.0 cm⁻¹ to the blue of the origin. The latter feature is assigned as ν_{10a} in this molecule.

(16) Herzberg, G. *Molecular Spectra and Molecular Structure*; Van Nostrand Reinhold: New York, 1966; Vol III, p 660. Other authors have referred to ν_{10a} as ν_{13} .

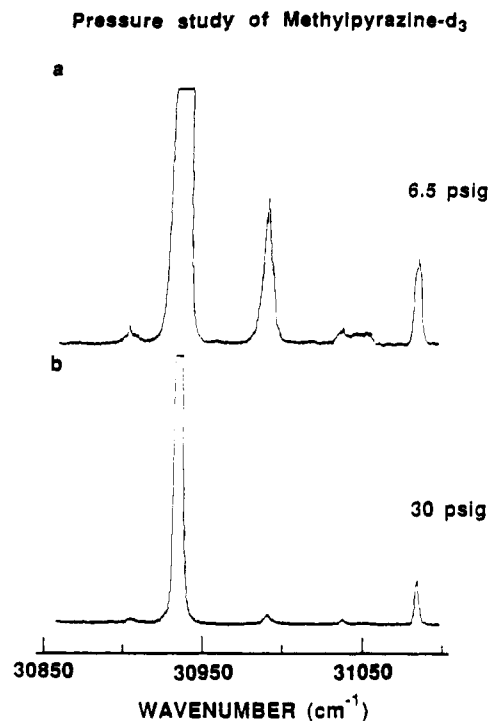


Figure 3. Expansion pressure study of methyl-*d*₃-pyrazine (**11**). The backing pressures applied are (a) 6.5 psig and (b) 30 psig. The peak near the origin has characteristic hot band behavior.

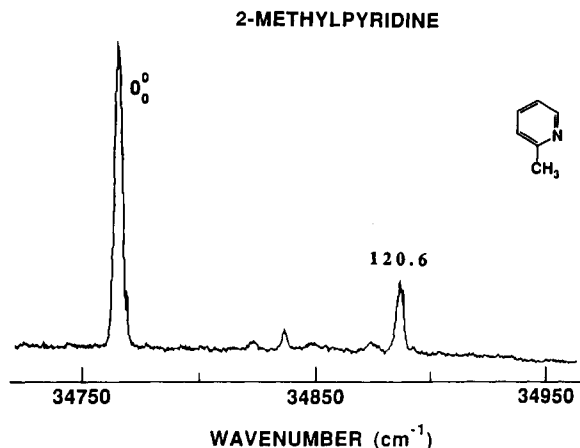


Figure 4. MRES of jet cooled 2-methylpyridine (**3**) around its 0_0^0 transition region. The intense origin occurs at 34766.5 cm⁻¹. The feature at 120.6 cm⁻¹ is assigned as the $16b_2^2$ vibronic transition. No methyl torsional transitions are observed in this spectrum.

Deuteration of the methyl group causes most of the weak features in the MRES to shift to higher energy, although a few do not shift at all. Only the first weak doublet feature (peaks B and C) displays an energy reduction upon methyl deuteration. From an expansion pressure study for both **2** and **11**, however, this doublet feature can be assigned as a vibrational hot band (see Figures 2 and 3). Deuteration of the methyl rotor should yield a significant isotope effect for the features associated with this isolated substituent: if the rotor is unhindered by a potential barrier (a "free rotor"), H/D isotope substitution should reduce the level spacings by a factor of 2; if the methyl motion is both hindered and isolated from the other molecular ring modes (usually a good assumption), H/D isotope substitution should reduce the level spacings by roughly a factor of $\sqrt{2}$. As the experimentally observed shifts are so small and not systematic, these features are not associated with pure methyl rotor transitions, either hindered or free.

The MRES of 2-methylpyridine (**3**) shown in Figure 4 is nearly identical with that of methylpyrazine. Neither the MRES of **2**

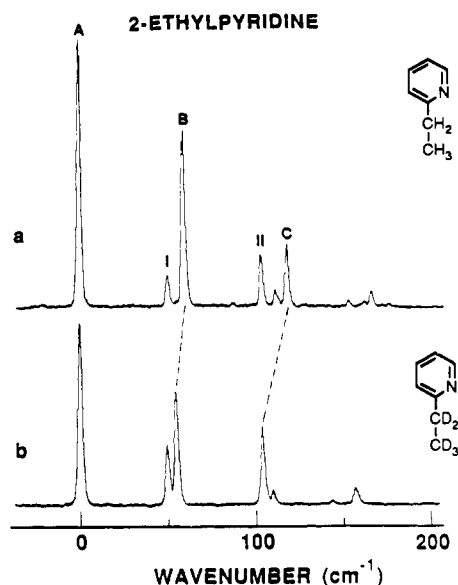
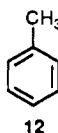


Figure 5. MRES of (a) 2-ethylpyridine (**5**) and (b) 2-ethyl-*d*₅-pyridine (**13**) around their 0_0^0 transition regions. The origins occur at 34 758.6 cm⁻¹ for **5** and at 34 764.2 cm⁻¹ for **13**. Only one origin is observed for each molecule. See Table I for assignments and positions.

nor that of **3** evidences obvious methyl rotor transitions. In contrast, the MRES of toluene (**12**) shows intense methyl free



rotor transitions in its origin region.^{9a,b} This difference between the spectrum of toluene and those of the three heterocycles **2**, **3**, and **11** must arise from the difference in the elemental composition and symmetry of the aromatic ring and thus the difference in the symmetry and strength of the rotational potential experienced by the methyl group; replacement of a ring C-H group with a nitrogen atom and its nonbonding electrons must change the potential energy barrier for methyl torsion.

Since no methyl torsional transitions are directly observed for **2**, **3**, and **11**, one cannot readily discern (from these data alone) whether the methyl potential barrier has increased or decreased for these heterocycles relative to the methyl potential barrier for toluene. The barrier to internal rotation of the methyl group in toluene has been established to be extremely small (ca. 10 cal/mol) by both experiment and theory.^{9,17} For 2-methylpyridine (**3**), the barrier to rotation has been reported to be 258 cal/mol as measured by microwave spectroscopy¹⁸ and 207 cal/mol as calculated by MINDO/3 semiempirical procedures.^{8a} MOPAC 5/PM3 calculations indicate a barrier of 54 cal/mol for 2-methylpyridine and 17 cal/mol for methylpyrazine. The MRES results for **2** are consistent with our calculations for this molecule and with the experimental and theoretical results for **3**.

The preponderance of experimental and theoretical data on barriers to internal methyl rotation for 2-methyl-substituted-1-*N*-heterocycles suggests that this barrier is considerably larger than that found for methyl-substituted benzenes.¹³ Three possible mechanisms could be responsible for this increased barrier to rotation: a reduced steric effect for the α -hydrogen(s) of the alkyl

(17) (a) Xie, Y.; Boggs, J. E. *J. Comput. Chem.* **1986**, *7*, 158 and references cited therein. (b) Kreiner, W. A.; Rudolph, H. D.; Tan, B. T. *Mol. Spectrosc.* **1973**, *48*, 86. (c) Rudolph, H. D.; Preizler, H.; Gaeschke, A.; Wendling, P. Z. *Naturforsch.* **1967**, *22A*, 940. (d) Dalling, D. K.; Ladner, K. H.; Grant, D. M.; Woolfenden, W. R. *J. Am. Chem. Soc.* **1977**, *99*, 7142. (e) Cavagnat, D.; Lascombe, J. *J. Mol. Spectrosc.* **1982**, *92*, 141. (f) Gough, K. M.; Henry, B. R.; Wildman, T. A. *J. Mol. Struct. (THEOCHEM)* **1985**, *124*, 71.

(18) Dretzler, H.; Rudolph, H. D.; Mäder, H. Z. *Naturforsch.* **1970**, *25*, 25.

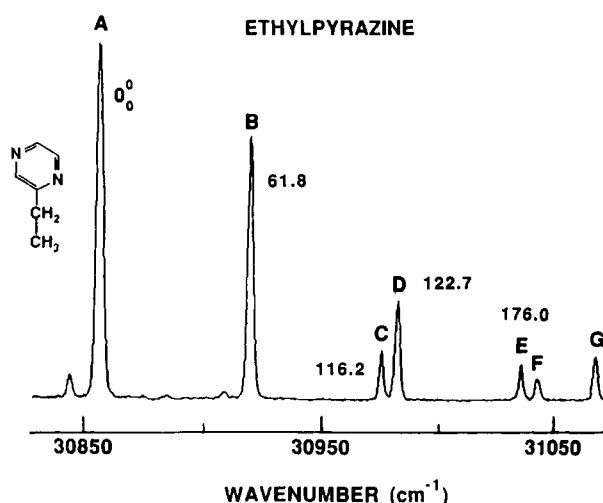


Figure 6. MRES of jet cooled ethylpyrazine around its 0_0^0 region. The origin occurs at 30 856.8 cm⁻¹ and a torsional progression of the ethyl group is built on it (see Table II for assignments and positions). Only one origin is identified in this spectrum.

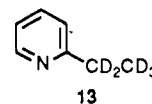
Table I. Positions for 2-Ethylpyridine and 2-Ethyl-*d*₅-pyridine Features in the 0_0^0 Region of the $S_1 \leftarrow S_0$ Transition (Figure 5)

| feature ^a | ethylpyridine $\nu - \nu(0_0^0)$, cm ⁻¹ | ethyl- <i>d</i> ₅ -pyridine $\nu - \nu(0_0^0)$, cm ⁻¹ | isotope shift, % |
|----------------------|--|---|---------------------|
| A | 0.0 (34 758.6) | 0.0 (34 764.2) | |
| B | 59.9 | 53.8 | 10.0 |
| C | 117.8 | 101.4 | 13.9 |

^a A through C are the notation for the observed vibronic features in the absorption spectrum of each molecule as shown in Figure 5.

substituent when directed toward the nitrogen lone pair electrons; asymmetric π and π^* interactions in the ring system;^{13a} and an increased attractive interaction between an α -hydrogen and the nitrogen lone pair (i.e., a "hydrogen bonding" interaction). Ab initio calculations on aldehyde imines¹⁹ suggest that the reason for this increased barrier is an attractive interaction between an alkyl group α -hydrogen and the nitrogen in-plane lone pair electrons. In subsequent discussions of the conformational analysis of 2-alkylpyridines and 2-alkylpyrazines, an attractive interaction between the nitrogen lone pair and an α -hydrogen atom will also be invoked.

B. Ethylpyrazine (4), 2-Ethylpyridine (5), and Related Ethyl-Substituted Heterocycles. The MRES about the origin region of the $S_1 \leftarrow S_0$ transition of 2-ethylpyridine (**5**) and 2-ethyl-*d*₅-pyridine (**13**) are presented in Figure 5, and that of



ethylpyrazine (**4**) is presented in Figure 6. These spectra, which are strikingly similar, can be interpreted in one of two ways: (a) each spectrum consists of one origin and a series of vibronic features built on it; or (b) each spectrum consists of two origins (the first two peaks A and B) and two series of vibronic features built on them.

We have previously used deuterated substrates to identify the 0_0^0 transitions in complex spectra, since the positions of origins do not shift relative to the lowest energy 0_0^0 transition while vibrations do have isotope effects (from 3 to 8% typically).⁹ In order to choose between these two spectroscopic assignments for **5**, a comparison can be made between the MRES of **5** and its deuterated analogue **13** (Figure 5). The MRES of **5** and **13** show an origin peak (A) at 34 758.6 and 34 764.2 cm⁻¹, respectively

(19) Dorigo, A. E.; Pratt, D. W.; Houk, K. N. *J. Am. Chem. Soc.* **1987**, *109*, 6591.

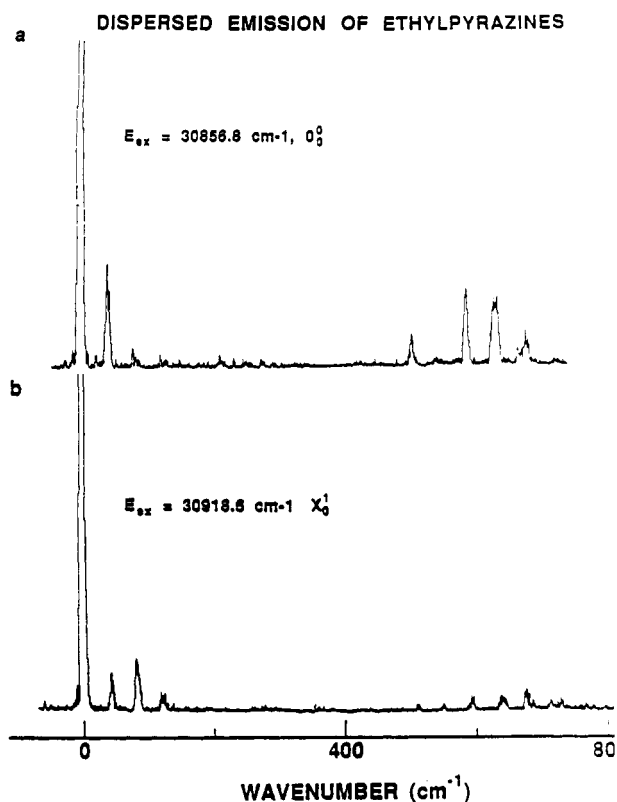


Figure 7. Dispersed emission spectra of ethylpyrazine: (a) excitation at 30856.8 cm⁻¹ (0.0 cm⁻¹), the feature marked A in Figure 6; (b) excitation at 30918.6 cm⁻¹ (0.0 cm⁻¹), the feature marked B in Figure 6.

(Figure 5). The features marked B and C are assigned as members of a vibrational progression related to the motion of the ethyl group based on their observed shift in energy relative to the 0₀⁰ transition upon deuteration of the ethyl group (see Table I). Features marked I and II in Figure 5a are most likely due to ring modes. We conclude that only one origin is observed in the absorption spectrum of 5.

Additionally, a distinction between these two possible assignments for the first two peaks in the MRES of ethylpyrazine (4) (marked A and B in Figure 6) can be made based on the dispersed emission spectra arising from excitation of these features. In a dispersed emission spectrum, an excited state (S₁) feature (vibronic or origin) is populated and emission from it is resolved. Figure 7 depicts the dispersed emission spectrum of ethylpyrazine excited at 30856.8 cm⁻¹ (0₀⁰ transition, Figure 7a) and at 30918.6 cm⁻¹ (X₀¹ transition, Figure 7b). Both spectra show the same spacing (40 cm⁻¹) of vibrational progressions built on the excitation line. This observation implies that the peak marked B in Figure 6 is a member of the vibrational progression built on the single origin at 30856.8 cm⁻¹ (peak A of Figure 6). If the feature X₀¹ (0.0 cm⁻¹) in Figure 7b were a new origin of a second ethylpyrazine conformation, emission spectra arising from the two excitations (0₀⁰ and X₀¹) would not be so similar. The data and assignments for the absorption spectrum are collected in Table II. Since only one origin is observed, only one stable conformation of ethylpyrazine exists in the ground state.

These results taken together strongly suggest that only a single origin (0₀⁰) transition is observed for 2-ethylpyridine and ethylpyrazine. As shown in Figure 8, several conformations can be considered as the possible stable ground state minimum observed for both ethylpyrazine and 2-ethylpyridine: perpendicular 14, syn-gauche and anti-gauche (15 and 16, respectively), and syn-planar and anti-planar (17 and 18, respectively). For ethylbenzene, C_β is in a plane perpendicular to the plane of the aromatic ring, i.e., τ(C_{ortho}-C_{ipso}-C_α-C_β) = 90° as in 14.^{9a,c} In these heterocycles, unlike ethylbenzene, 15 and 16 are not identical and hence have different energies; similarly, conformers 17 and 18 are not energetically degenerate. To determine which of these five conformations corresponds to the single 0₀⁰ transition observed, we

Table II. Positions for Ethylpyrazine Features in the 0₀⁰ Region of the S₁ ← S₀ Transition (Figure 6)

| feature ^a | ν - ν(0 ₀ ⁰), cm ⁻¹ | assignment ^b |
|----------------------|---|---------------------------------|
| A | 0.0 (30856.8) | origin |
| B | 61.8 | T ₀ ¹ |
| C | 116.2 | I |
| D | 122.7 | T ₀ ² |
| E | 176.0 | I + T ₀ ¹ |
| F | 183.1 | T ₀ ³ |
| G | 207.9 | II |

^aA through G are the notations of Figure 6 for the observed vibronic features in the absorption spectrum of ethylpyrazine. ^bI and II are the notation for the undetermined vibrational motion of the molecule, and T is the notation for the torsional vibrational motion of the ethyl group (see Figure 6).

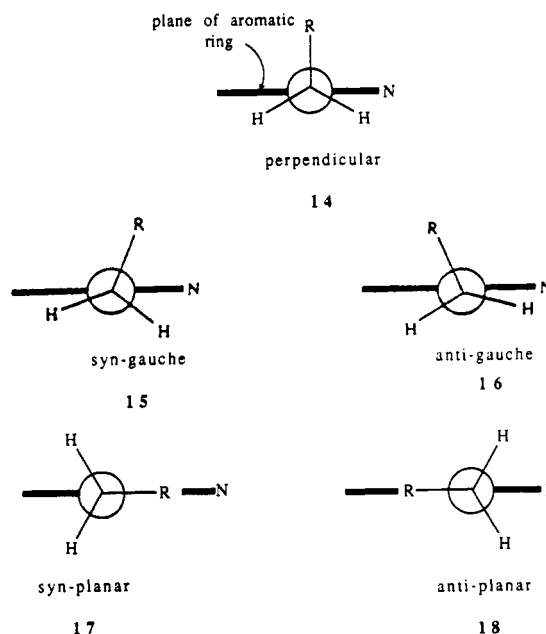
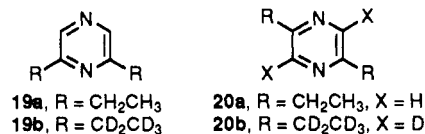


Figure 8. Possible conformations of ethylpyridine and ethylpyrazine (R = CH₃). The assignments "syn" and "anti" refer to the relative position of the nitrogen atom and the R = CH₃ substituent.

have (a) obtained the MRES of 2,6-diethylpyrazine (19a) and 2,5-diethylpyrazine (20a) and their deuterated analogues 19b and 20b and, (b) performed a series of MOPAC 5/PM3 calculations



on ethylpyrazine and 2-ethylpyridine. As described above, the deuterated derivatives are used in the MRES experiments to distinguish between origin transitions, which do not show isotope shifts, and vibrational transitions, which do show isotope shifts, relative to the MRES of the parent compound.

Figure 9 shows the MRES of jet cooled 2,6-diethylpyrazine (19a) and its *d*₁₀-analogue 19b about the origin region of the S₁ ← S₀ transition. A comparison of these two spectra demonstrates that two origins are observed for each molecule, at 30949.6 (A) and 30962.6 (B) cm⁻¹ for 19a, and at 30962.6 (A') and 30975.1 (B') cm⁻¹ for 19b. Comparison of Figure 9 with Figures 5 and 6 indicates that many of the single features in the ethylpyrazine and 2-ethylpyridine spectra are doubled in the diethylpyrazine spectra, as would be expected if one conformer were present for ethylpyrazine and two conformers were present for 2,6-diethylpyrazine. The same vibronic features found in the spectrum of ethylpyrazine also appear to be built on each of these origins. Since two origins are observed for both 19a and 19b, each of these molecules has two stable conformers in the ground state. These results are consistent with a single nonplanar conformation for

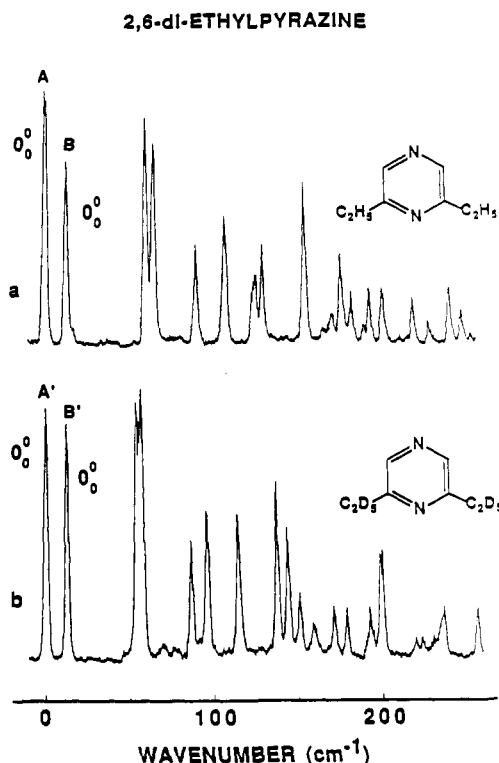


Figure 9. MRES of the 0_0^0 region of the ($S_1 \leftarrow S_0$) transition for jet cooled (a) 2,6-diethylpyrazine (**19a**) and (b) 2,6-diethyl- d_{10} -pyrazine (**19b**). Two origins are observed for both **19a** and **19b**. The origins occur at 30949.6 and 30962.6 cm^{-1} for **19a** and at 30962.6 and 30975.1 cm^{-1} for **19b**.

the ethyl group on these heterocycles; i.e., $\tau(\text{N}-\text{C}_2-\text{C}_\alpha-\text{C}_\beta) \neq 0$ or 180° .

The MRES of 2,5-diethylpyrazine (**20a**) and its deuterated analogue 2,5-diethylpyrazine- d_{12} (**20b**) are shown in Figure 10. Only the first feature in each spectrum can be assigned as an origin transition because all the other peaks show significant relative isotope effects. Nonetheless, from the above discussion concerning the conformation of ethyl groups relative to the plane of the aromatic ring, two origins transitions (as found for **19** and 1,4- and 1,3-diethylbenzenes^{9a,c}) are to be expected. Note that the two origins for 2,6-diethylpyrazine (**19a**) are separated by 13.0 cm^{-1} ; this separation can be compared with the smaller separations of 4 and 10 cm^{-1} found for the two origins of 1,4-diethylbenzene and 1,3-diethylbenzene, respectively.^{9a,c} Apparently, the two origins for **20a** (and **20b**) must be degenerate. The change in the comparable meta/para substitution splitting for the benzene ring system is only ca. a factor of 2.5 (10 versus 4 cm^{-1}), while it is significantly greater for the pyrazine ring system (13 versus <2 cm^{-1}). Since the meta splittings for the two ring systems are similar (10 versus 13 cm^{-1}) while the para splittings are quite different, we suggest that the coupling between the two ethyl groups is an electronic rather than a steric effect and that the ring-mediated substituent coupling in the (para) 2,5-diethylpyrazine is suppressed relative to that for 1,4-diethylbenzene.

Figure 11 illustrates the PM3-derived potential energy function for ethylpyrazine about $\tau_1 = \tau(\text{N}-\text{C}_{\text{ipso}}-\text{C}_\alpha-\text{C}_\beta)$. A single energy minimum is observed at ca. $\tau_1 = 103^\circ$, the anti-gauche conformer **16**. The single energy minimum at ca. 90° is consistent with the above reported results on **4**, **5**, **13**, **19**, and **20**. Note that for the ethyl-substituted benzenes, the energy minimum is found to be at $\tau_1 = 90^\circ$.

We thus conclude that the ethyl group of ethylpyrazine and 2-ethylpyridine is not truly perpendicular to the plane of the ring. The deviation of τ_1 by roughly 10° to 15° from a true perpendicular conformation ($\tau_1 = 90^\circ$) for the $\text{C}_\alpha-\text{C}_\beta$ bond with respect to the plane of the ring is suggested, based on ab initio calculations¹⁷ as discussed above for 2-methylpyridine and methylpyrazine, to be due to a ring nitrogen lone pair electron/ α -hy-

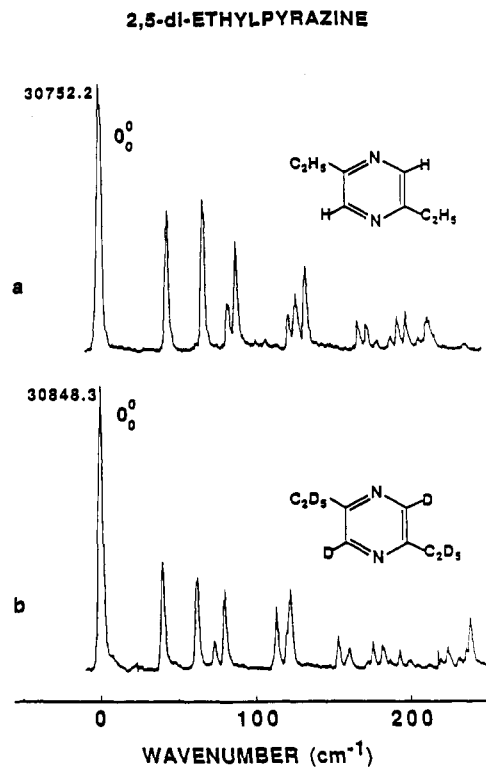


Figure 10. MRES of the 0_0^0 region of the ($S_1 \leftarrow S_0$) transition for jet cooled (a) 2,5-diethylpyrazine (**20a**) and (b) 2,5-diethyl- d_{10} -pyrazine- d_2 (**20b**). The transition energies for the observed 0_0^0 transitions of **20a** and **20b** are marked on the figure.

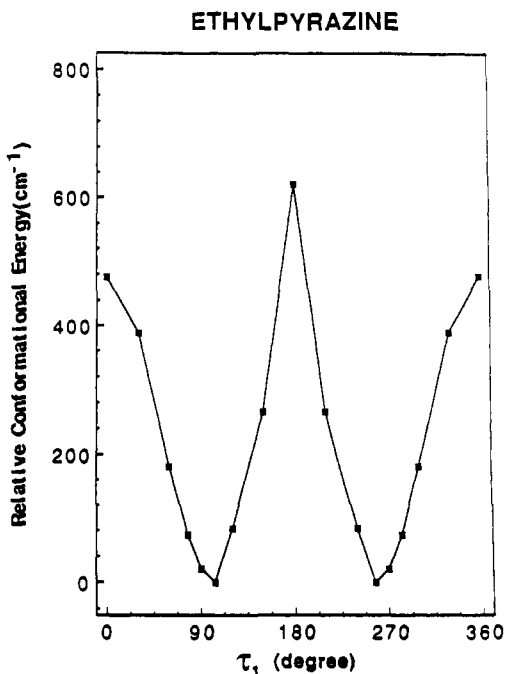
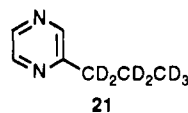


Figure 11. The PM3 conformational energy profile for ethylpyrazine along the conformational coordinate $\tau_1 = \tau(\text{N}-\text{C}_{\text{ipso}}-\text{C}_\alpha-\text{C}_\beta)$. The conformational energies are obtained by fixing τ_1 at the given value and optimizing the other coordinates (see **10b**).

drogen interaction. This interaction results in an ethyl α -hydrogen moving toward the ring plane and thereby generating an overall anti-gauche **16** conformation for these molecules.

C. Propylpyrazine (6), 2-Propylpyridine (7), and Related Compounds. The MRES of propylpyrazine (**6**), its deuterated derivative propyl- d_7 -pyrazine (**21**), and 2-propylpyridine (**7**) are shown in Figures 12a, 12b and 13, respectively. The spectra of **6** and **7** are similar, with that of **7** being much weaker, presumably



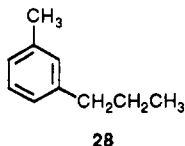
due to the reduced lifetime of its S_1 state through relatively enhanced nonradiative processes (i.e., intersystem crossing and internal conversion).

To distinguish between origin (0_0^0) transitions and vibrations, the isotope shifts are determined in the MRES of **21** relative to **6**. Only one of the peaks (marked A') among the features in Figure 12 does not show a relative isotope shift. Other features show approximately a 5% isotope effect (B, C, D, and E) or a 9% isotope effect (B' and C'). These data are collected in Table III. The two peaks A and A' (at 30782.3 and 30852.0 cm^{-1} , respectively) in the MRES of propylpyrazine which have no relative isotope effect ($E_A - E_{A'} = 70 \text{ cm}^{-1}$) are assigned as origins. The peaks marked B, C, D, and E are assigned as the torsional mode vibrational progression associated with propyl group motion built on origin A, and those marked B' and C' are assigned as a similar torsional mode vibrational progression built on origin A'. The observations of two origins implies that two stable conformers exist for the ground state of propylpyrazine.

From the MRES of jet cooled 2-propylpyridine (**7**) (Figure 13), the number of origin transitions is not readily assignable. Since two origins are observed in the MRES of propylpyrazine, by analogy two origins would be predicted in the MRES of 2-propylpyridine. In Figure 13, the peaks at 34665.6 cm^{-1} (A) and at 34703.1 cm^{-1} (A') are assigned as origins for two different conformations. Based on this assignment, other peaks are assigned as shown in Table IV.

To define the conformational properties of propyl-substituted aromatic compounds, e.g., propylpyrazine and 2-propylpyridine, two torsional degrees of freedom must be assigned, τ_1 and τ_2 as shown in Figure 14a. By analogy with the benzene \rightarrow toluene \rightarrow ethylbenzene \rightarrow propylbenzene series,^{9a-c} and by analogy with the results found for ethylpyrazine and 2-ethylpyridine discussed above, we assign $\tau_1 = \tau(\text{N}-\text{C}_{\text{ipso}}-\text{C}_\alpha-\text{C}_\beta) \approx 103^\circ$ for **6**, **7**, and **21** (cf. **22-24** in Figure 14a). The conformations depicting τ_2 are **22-24** and are also shown in Figure 14a.

The experimental results for propylpyrazine (**6**) and 2-propylpyridine (**7**) should be related to those found for 3-methylpropylbenzene (**28**); however, two origins are found ex-



perimentally in the MRES of **6** and **7** while three origins representing the conformations **25-27** (cf. Figure 14b) are observed for 3-methylpropylbenzene.^{9a,b} The situation for **6** and **7** is somewhat different from that for **28** because the asymmetric perturbation of the latter molecule is a methyl substituent while it is the ring nitrogen(s) in the former two substrates.

The following three possibilities arise for the two assigned origins in the spectra of **6** and **7**: (a) one gauche (**23** or **24**) and the anti conformation **22** are observed; (b) anti **22** and both gauche **23** and **24** (coincidentally degenerate in energy) are observed; or (c) only both gauche (**23** and **24**) conformations are observed.

To aid in the conformational assignments, we examine a substrate having an additional substituent which enhances the ring's asymmetry. For example, while propylbenzene evidences two 0_0^0 transitions (one each for the anti and the gauche conformers),^{9a,d} 3-methylpropylbenzene shows three 0_0^0 transitions (one for the anti **25** and one each for the gauche **26** and **27** conformers).^{9a,d} Relative to propylpyrazine, 2-methyl-6-propylpyrazine (**29**) fits this

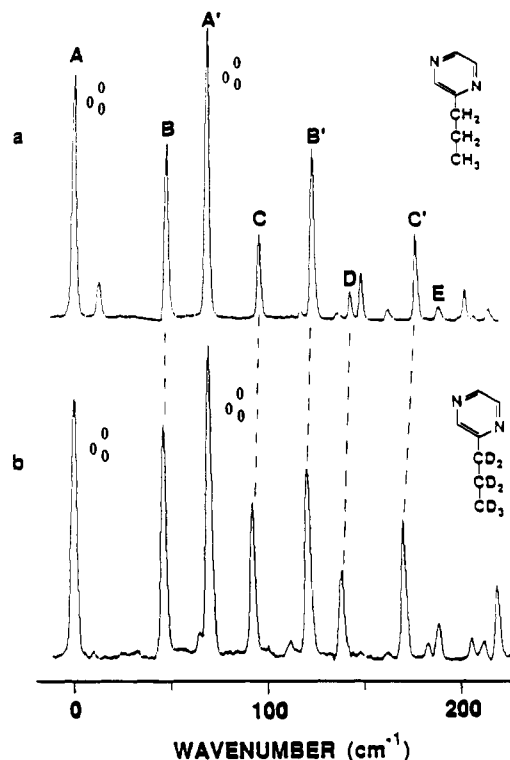
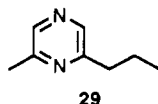


Figure 12. MRES of jet cooled (a) propylpyrazine (**6**) and (b) propyl- d_7 -pyrazine (**21**) around their 0_0^0 regions. The peaks marked A and A' are assigned as the origin transitions of different conformers based on the absence of a relative isotope effect (see Table III).

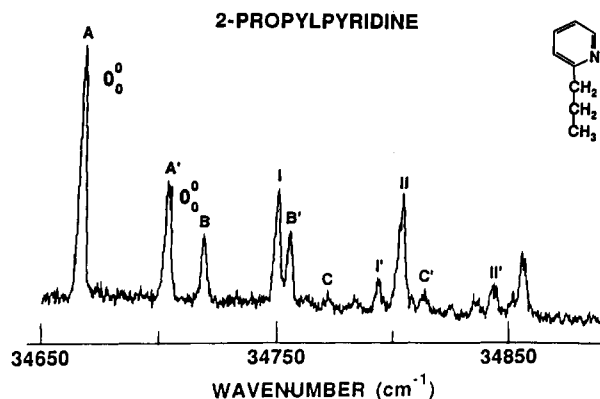


Figure 13. MRES of jet cooled 2-propylpyridine (**7**) around its 0_0^0 transition region. The peaks marked A (34665.5 cm^{-1}) and A' (34703.1 cm^{-1}) are assigned as the origin transitions of two conformers. See Table IV for assignments and positions of the transitions.

Table III. Positions for Propylpyrazine and Propyl- d_7 -pyrazine Features in the 0_0^0 Region of the $S_1 \leftarrow S_0$ Transition (Figure 12)

| feature ^a | propylpyrazine $\nu - \nu(0_0^0)$, cm^{-1} | propyl- d_7 -pyrazine $\nu - \nu(0_0^0)$, cm^{-1} | isotope shift, % |
|----------------------|---|--|---------------------|
| A | 0.0 (30782.3) | 0.0 (30787.3) | |
| B | 48.5 | 46.1 | 4.9 |
| C | 97.4 | 92.4 | 5.1 |
| D | 145.6 | 138.3 | 5.0 |
| E | 193.0 | 183.0 | 5.0 |
| A' | 0.0 (30852.0) | 0.0 (30857.5) | |
| B' | 56.0 | 50.8 | 9.3 |
| C' | 111.2 | 100.7 | 9.4 |
| D' | | 149.5 | |

^a A through E and A' through D' are the notation for the observed vibronic features for each conformer of each molecule (see Figure 12).

strategy, in that both the methyl group and the ring nitrogens are asymmetrically disposed relative to the propyl group. Hence, 2-methyl-6-propylpyrazine was prepared and its MRES obtained. In principle, the added methyl group should break any degeneracy

Table IV. Positions for 2-Propylpyridine Features in the 0_0^0 Region of the $S_1 \leftarrow S_0$ Transition (Figure 13)

| feature ^a | $\nu - \nu(0_0^0)$, cm^{-1} | assignment ^b |
|----------------------|---------------------------------------|-------------------------|
| A | 0.0 (34 665.6) | origin I |
| B | 52.7 | 1_0^1 |
| C | 105.6 | 1_0^2 |
| I | 83.4 | 2_0^1 |
| II | 137.0 | 3_0^1 |
| A' | 0.0 (34 703.1) | origin II |
| B' | 51.3 | 1_0^1 |
| C' | 104.9 | 1_0^2 |
| I' | 89.6 | 2_0^1 |
| II' | 139.4 | 3_0^1 |

^a A through C and I, II are the notations for the observed vibronic features in one conformer of 2-propylpyridine; A' through C' and I', II' are notations for the observed vibronic features in the other conformer of this molecule (see Figure 13). ^b 1 through 3 and I' through 3' are the notations for the undetermined vibrational motion of the molecule for each stable conformation (see Figure 13).

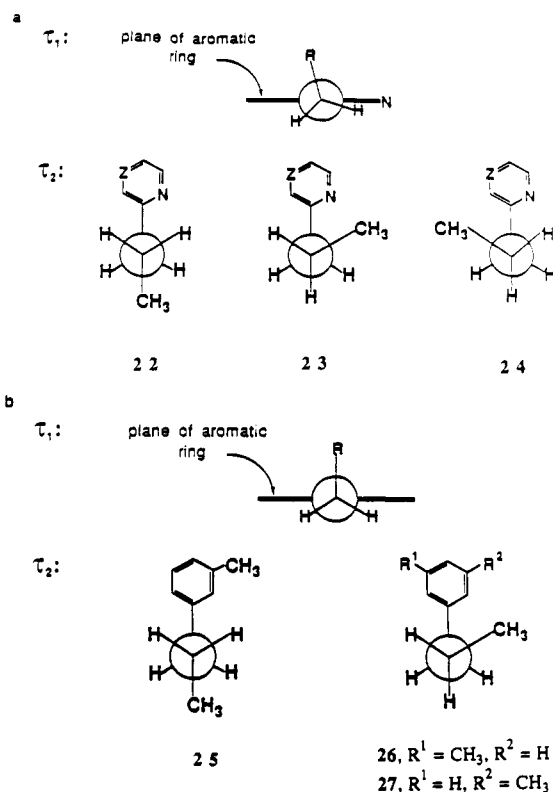


Figure 14. (a) Possible conformations of propylpyrazine ($Z = \text{N}$) and 2-propylpyridine ($Z = \text{CH}$) about $\tau_1 = \tau(\text{N}-\text{C}_{\text{ipso}}-\text{C}_\alpha-\text{C}_\beta)$ and $\tau_2 = \tau(\text{C}_{\text{ipso}}-\text{C}_\alpha-\text{C}_\beta-\text{C}_\gamma)$. (b) Conformations of 3-methylpropylbenzene about $\tau_1 = \tau(\text{C}_{\text{ortho}}-\text{C}_{\text{ipso}}-\text{C}_\alpha-\text{C}_\beta)$ and $\tau_2 = \tau(\text{C}_{\text{ipso}}-\text{C}_\alpha-\text{C}_\beta-\text{C}_\gamma)$.

in the energy of the 0_0^0 transitions of the gauche conformers.

The origin region of the $S_1 \leftarrow S_0$ of 2-methyl-6-propylpyrazine (**29**) is shown in Figure 15. The MRES of **6**, **7**, and **29** are very similar, as indicated by the letters A–D and A'–C' identifying the various transitions shown in Figures 12 and 15. Thus the spectrum of **29** as presented in Figure 15 evidences only two origins, A and A' (at 30 984.3 and 31 059.8 cm^{-1} , respectively), with the same vibrational progressions built on them. Several other weak features due to methyl substitution can be observed in the spectrum as well. Since only two origins can be assigned, excluding the possibility of degenerate origin transitions, the data suggest that **29** has only two stable conformers in the ground state.

To distinguish between the two other possibilities given above is not easy, especially as previous results in the benzene series and chemical intuition do not particularly favor either of them over the other. MOPAC 5/PM3 calculations performed on propylpyrazine are summarized in Figure 16. Three energy minima are located, namely, the anti conformation **22** and the syn-gauche **23** and the anti-gauche **24** (Figure 14a, $Z = \text{N}$). The relative

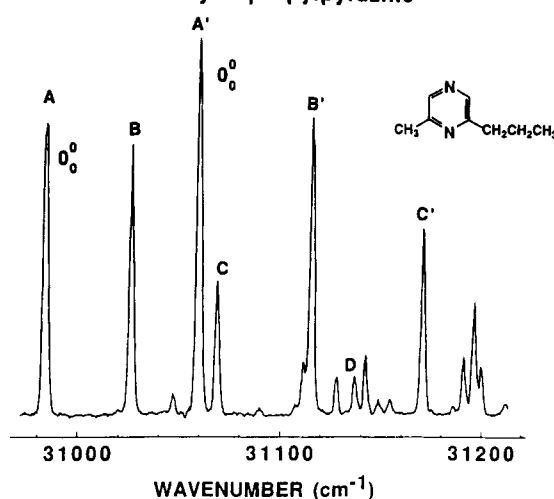
2-Methyl-6-propylpyrazine

Figure 15. MRES of jet cooled 2-methyl-6-propylpyrazine (**29**) around its 0_0^0 region. Two origins are identified - at 30 984.3 and 31 059.8 cm^{-1} . Torsional vibrational progressions are built on each origin. This spectrum is similar to that of propylpyrazine (**6**) as shown in Figure 12.

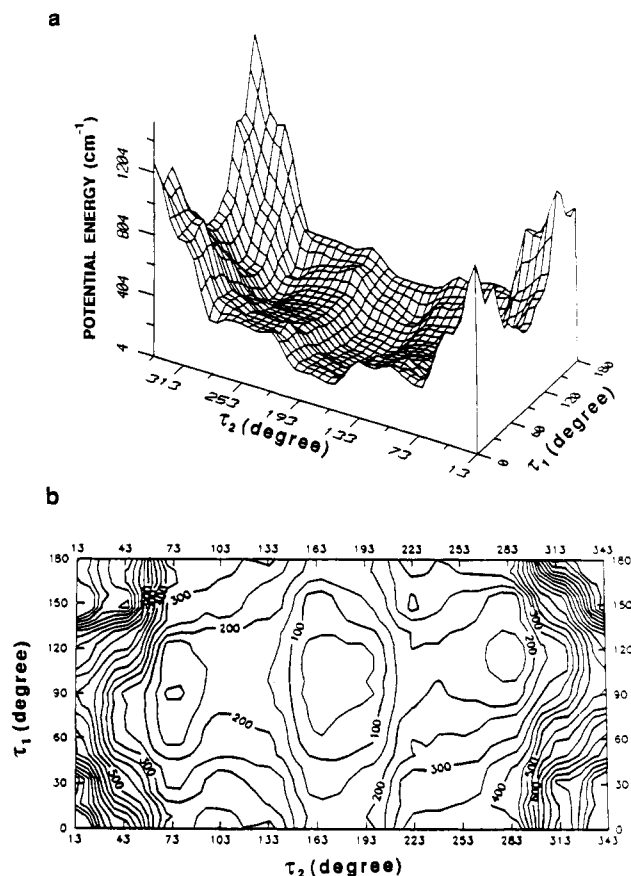


Figure 16. The PM3 calculated conformational energy surface of propylpyrazine along the conformational coordinates $\tau_1 = \tau(\text{N}-\text{C}_{\text{ipso}}-\text{C}_\alpha-\text{C}_\beta)$ and $\tau_2 = \tau(\text{C}_{\text{ipso}}-\text{C}_\alpha-\text{C}_\beta-\text{C}_\gamma)$: (a) three-dimensional surface and (b) two-dimensional contour map. The values of the conformational energy are relative to that for the anti conformer of propylpyrazine. Three energy minima are shown: ($\tau_1 = 111^\circ$, $\tau_2 = 180^\circ$), ($\tau_1 = 87^\circ$, $\tau_2 = 75^\circ$), and ($\tau_1 = 111^\circ$, $\tau_2 = 287^\circ$).

energies of these three conformations are shown in Figure 16 along with the values of τ_1 and τ_2 for these conformations. The calculations suggest three stable conformations of similar energy, with the anti conformer lower in energy (by about 2 kcal/mol) than the two gauche conformers. Pending additional experimental and/or theoretical studies, we can only speculate as to the conformational preferences of propylpyrazines and 2-propylpyridine;

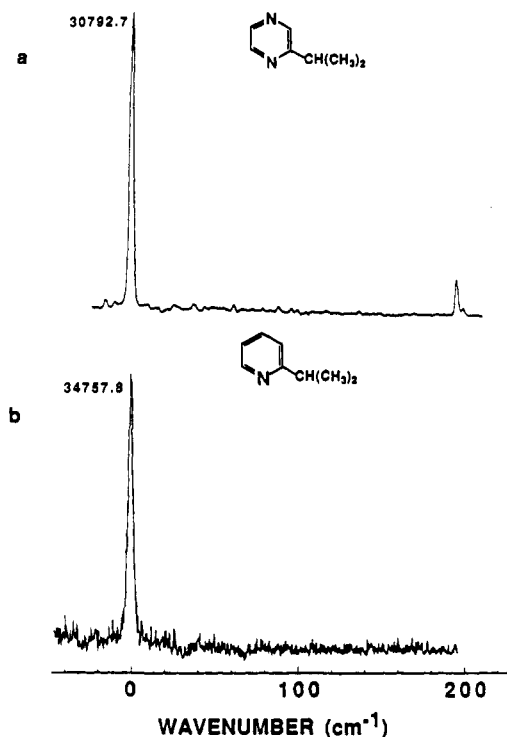


Figure 17. MRES of jet cooled (a) isopropylpyrazine (8) and (b) 2-isopropylpyridine (9) around their origin transition region.

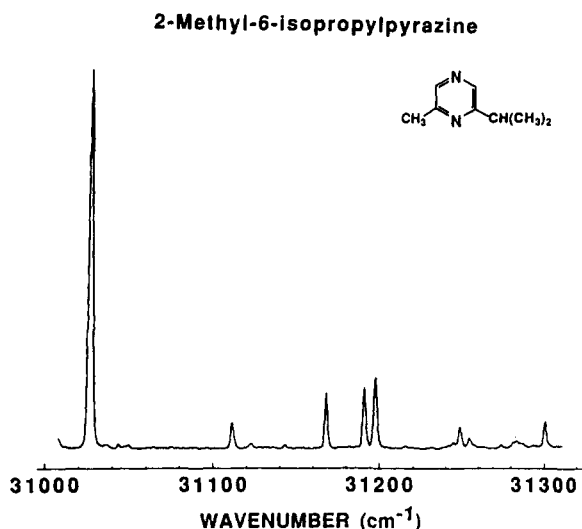


Figure 18. MRES of the 0° region of ($S_1 \leftarrow S_0$) for jet cooled 2-methyl-6-isopropylpyrazine (30). The single intense feature is assigned as the origin and occurs at 31027.4 cm^{-1} .

however, results for benzene analogues and MOPAC calculations suggest that one of the stable observed conformers should be the anti **22**.

D. Isopropylpyrazine (8), 2-Isopropylpyridine (9), and 2-Methyl-6-isopropylpyrazine (30). The MRES of jet cooled isopropylpyrazine (8) and 2-isopropylpyridine (9) are depicted in Figure 17, a and b, respectively. Only one intense origin is observed (at 30792.7 and 34757.8 cm^{-1} , respectively) in each spectrum. Thus, only one stable conformer exists for these molecules in the ground state.

To probe the conformations of the isopropylazines further, 2-methyl-6-isopropylpyrazine (30) is examined and Figure 18

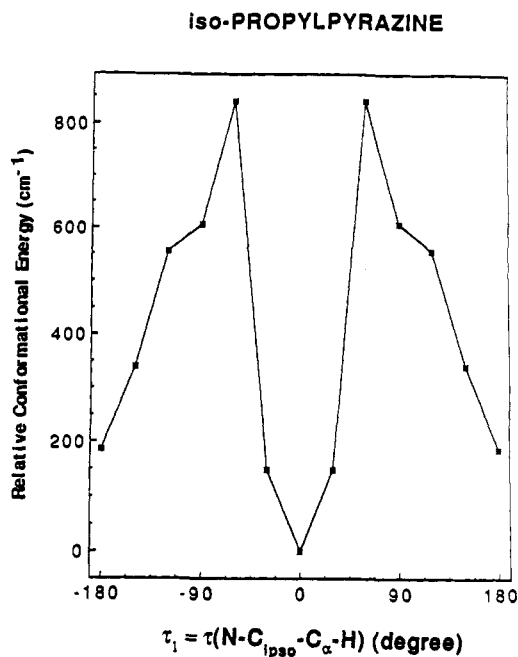
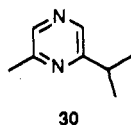
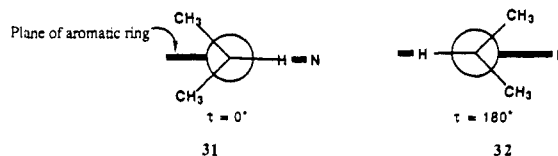


Figure 19. The PM3 conformational energy profile for isopropylpyrazine along the conformational coordinate $\tau_1 = \tau(\text{N}-\text{C}_{\text{ipso}}-\text{C}_{\alpha}-\text{H})$.

displays its MRES around the origin region of the $S_1 \leftarrow S_0$ transition. The MRES of **30** contains only one origin with several weak features to high energy built on it. This observation implies that only one stable conformer exists for **30** in the ground state.

The conformation of isopropylbenzene for which the α -hydrogen is in the plane of the ring has been determined to be the stable minimum energy conformation. From this result, one of the two conformers **31** or **32** can be considered as the single stable con-



formation of isopropylpyrazine. Because of the demonstrated asymmetric interaction of the substituent with the ring, these two conformers do not have the same conformational energy. Conformer **31** for which the α -hydrogen is toward the nitrogen atom and nearly in the plane of the ring is suggested to be the minimum energy conformer based on the foregoing results for methyl, ethyl, and propyl pyridines and pyrazines and MOPAC 5/PM3 calculations²⁰ for isopropylpyrazine (see Figure 19).

The current literature consensus^{4,8,21} for these molecules appears to be that $\tau_1(\text{N}-\text{C}_2-\text{C}_{\alpha}-\text{H}_{\alpha}) = 0^{\circ}$ or 180° ; that is, H_{α} lies in the plane of the aromatic ring, for a 2-isopropyl-3-unsubstituted pyridine. Note, however, that one report of a gauche ($\tau_1 = 60^{\circ}$) 2-isopropyl-3-unsubstituted pyridine has appeared.²² This latter study employs lanthanide shift reagents and NMR techniques. The relationship between ground state conformation and complexation (which may alter the observed geometry) with a lanthanide shift reagent requires a Curtin-Hammett/Winstein-Holness analysis^{23,24} not presented for the lanthanide shift studies.²²

(20) (a) In contrast to the MOPAC 5/PM3 results, MINDO/3 semi-empirical all-valence electron calculations have indicated^{8c} that the most stable conformation of 2-isopropylpyridine is $\tau(\text{N}-\text{C}_2-\text{C}_{\alpha}-\text{H}_{\alpha}) = 180^{\circ}$. (b) See also: Tower, J. L.; Spangler, L. H.; Pratt, D. W. *J. Am. Chem. Soc.* **1988**, *110*, 1615.

(21) Nilsson, I.; Berg, U.; Sandström, J. *Acta Chem. Scand.* **1984**, *B38*, 491.

(22) Uncuta, C.; Balaban, T.-S.; Gheorghiu, M. D.; Stanesco, L.; Petride, A.; Balaban, A. T. *Tetrahedron Lett.* **1985**, *26*, 4673.

(23) Seeman, J. I. *Chem. Rev.* **1983**, *83*, 83.

(24) Seeman, J. I.; Secor, H. V.; Hartung, H.; Galzerano, R. *J. Am. Chem. Soc.* **1980**, *102*, 7741.

III. Summary and Conclusions

This report presents one of the few experimental studies of the conformations of alkyl-substituted pyridines and pyrazines. The effect of the nitrogen atom on the conformational properties of 1-N-2-substituted azines can be evaluated and characterized through comparison with the isostructurally substituted benzene species.

The stable conformations of alkyl-substituted pyrazine and pyridine systems are determined through the use of supersonic jet mass resolved and fluorescence excitation spectroscopies and semiempirical (MOPAC 5/PM3) calculations. Under the conditions of the laser jet experiments, spectroscopic transitions are observed for the stable ground state conformations of these alkyl-substituted azines. Using specifically (positionally and isotopically) substituted derivatives and structural "logic", one can assign the geometry of these stable conformations. The individual stable conformations of these heterocycles are quite different from those of the comparable alkyl-substituted benzenes. One can draw the following four conclusions from the experimental and theoretical result reported above.

1. The motion of the methyl group in 2-methylpyridine and methylpyrazine is highly hindered in both S_0 and S_1 . Since methyl group behavior for toluene in both electronic states is nearly that of a free rotor, the potential surface for methyl motion in the azines and the benzenes is very different.

2. Spectroscopic studies yield single unique conformations (origins) for both 2-ethylpyridine and ethylpyrazine but yield two conformations (origins) for both 2,6-diethylpyridine and 2,6-diethylpyrazine. Based on semiempirical calculations, the ethyl substituents in these compounds are suggested to be somewhat tilted from the perpendicular with an α -hydrogen atom nearly in the plane of the aromatic ring [i.e., $\tau_1(\text{N}-\text{C}_2-\text{C}_\alpha-\text{H}_\alpha) \approx 17^\circ$]. This is to be contrasted with the reported minimum energy structure for ethylbenzene [i.e., $\tau_1(\text{C}_{\text{ortho}}-\text{C}_{\text{ipso}}-\text{C}_\alpha-\text{H}_\alpha) \approx 30^\circ$].

3. Two spectroscopic origins are observed for each propyl-substituted azine studied (2-propylpyridine, propylpyrazine, and the corresponding 2-methyl-6-propylazines). Excluding the possibility of degenerate origin transitions, two conformers are assigned for each of these molecules: one of the possible gauche conformers and the (most stable) anti conformer. For these compounds, a tilted conformation of the propyl group is suggested in which $\tau_1(\text{N}-\text{C}_2-\text{C}_\alpha-\text{H}_\alpha) \approx 17^\circ$. This result is in contrast to those of 3-methyl-1-propylbenzene for which three conformations are assigned: two gauche and one anti.

4. Only a single stable conformation is characterized for the isopropyl group in 2-isopropylpyridine and isopropylpyrazine. The assigned structure has the α -hydrogen atom of the isopropyl group lying in the plane of the aromatic ring pointing toward the ring nitrogen atom [i.e., $\tau_1(\text{N}-\text{C}_2-\text{C}_\alpha-\text{H}_\alpha) = 0^\circ$].

The combined available experimental and theoretical data for these molecules suggest that a relatively strong and important interaction exists between the α -hydrogen of the alkyl substituent and the ring nitrogen lone pair of electrons. This suggestion is reasonable: the nitrogen atom has a large negative partial charge, especially on the basis of Bader's integrated populations, and the α -hydrogens (i.e., $\text{C}_\alpha-\text{H}_\alpha$) have a substantial positive partial charge.

IV. Experimental Procedures

A. Spectroscopy and Calculations. All the spectra were obtained using two-color, two-photon ionization with time-of-flight mass detection. The MRES chamber is described elsewhere.¹⁵ A pulsed molecular jet was employed using an R.M. Jordan pulsed valve. All the samples were placed inside the valve head and heated to about 60 °C to increase their concentration in the beam. In all cases, helium was used as the carrier gas at roughly 50 psig. Two Nd³⁺/YAG lasers were used to produce excitation and ionization photons. The doubled output of DCM dye was employed for the $\pi^* \leftarrow n$ excitation of alkyl-substituted pyrazines, and the doubled output of R610 dye was employed for the $\pi^* \leftarrow n$ excitation of alkyl-substituted pyridines. For both systems the doubled output of R590 dye mixed with the residual 1.064 μm Nd³⁺/YAG beam was used to provide the ionization photon.

Dispersed emission (DE) experiments were performed in a fluorescence excitation (FE) chamber described previously.¹⁵ Expansion of the

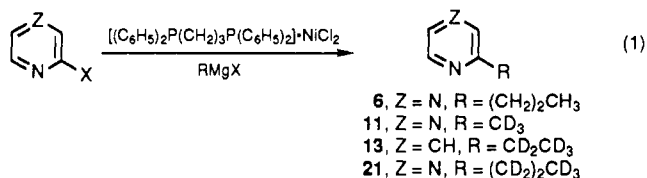
gas into the chamber was achieved with a CW nozzle with 100 μm pinhole. $f/4$ optics were used to collect and focus the emission onto the slits of an $f/8$ 2051 GCA McPherson monochromator. Spectra were recorded with a 1200 groove/mm, 1.0 μm blazed grating in the third order.

Stable geometries of various alkyl-substituted pyrazine and pyridine systems were calculated using the MOPAC 5 programs, which have two Hamiltonians available for structure calculations: PM3²⁵ and AM1.²⁶ The PM3 Hamiltonian has been augmented and improved for heteroatom (N, O, etc.) calculations. All calculational results reported in this work are based on the PM3 Hamiltonian. Input data for the calculations were obtained from the crystal structures of pyrazine²⁷ and normal alkanes²⁸ and the gas phase structure of pyridine.²⁹

2-Methylpyridine, 2-ethylpyridine, 2-propylpyridine, methylpyrazine, and ethylpyrazine were purchased from Aldrich. 2-Isopropylpyridine and isopropylpyrazine were obtained from Wiley Chemical Co. Grignard reagents and diethylzinc were obtained from Aldrich.

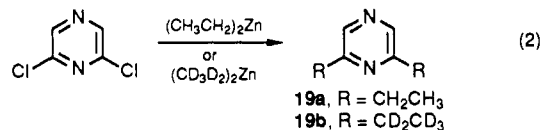
B. Synthesis of Substituted Pyridines and Pyrazines. General Approach and Methods. Crucial to the spectroscopic studies which follow is the use of a number of substituted azines chosen to satisfy certain symmetry and conformational requirements. In addition, a number of these compounds had to be prepared having specific isotopic substitution patterns. Because of the essential role of these substrates, and because they are not commercially available, it is useful to discuss the general strategies used to synthesize these compounds. Although several of the required substrates have been previously reported in the literature, in some cases the compounds were not expeditiously prepared or had been obtained as side products in, for example, mechanistic studies. The following discussion will focus attention on either new synthetic routes or improvements in previously reported methodologies.

Equation 1 illustrates the procedure by which four substrates, meth-



yl-*d*₃-pyrazine (11), propylpyrazine (6), propyl-*d*₇-pyrazine (21), and 2-ethyl-*d*₅-pyridine (13), can be prepared. For the pyrazines, the halogen of chloropyrazine is exchanged with the appropriate alkyl group using a cross-coupling reaction with the appropriate Grignard reagent in a reaction catalyzed by 1,3-bis(diphenylphosphino)propanedichloronickel(II) (Ni-Dppp).^{30,31} Similarly, 13 can be prepared by a cross-coupling reaction between 2-bromopyridine and ethyl-*d*₅-magnesium bromide.

2,6-Diethylpyrazine (19a) forms spontaneously at room temperature in the reaction of diethylzinc with 2,6-dichloropyrazine in toluene employing 1,3-bis(diphenylphosphino)propanedichloronickel(II) as a catalyst (eq 2). 2,6-Diethyl-*d*₁₀-pyrazine (19b) was similarly prepared in 69%



yield by the reaction of 2,6-dichloropyrazine with diethylzinc-*d*₁₀. Diethylzinc-*d*₁₀ was prepared from iodoethane-*d*₅, bromoethane-*d*₅, and ZnCu couple. This represents a significant improvement over a method reported by Ohta et al.³² in which ether and a palladium catalyst were used.

(25) (a) Stewart, J. J. *J. Comput. Chem.* **1989**, *10*, 209. (b) Stewart, J. J. *J. Comput. Chem.* **1989**, *10*, 221.

(26) (a) Dewar, M. J. S.; Zoebisch, E. G.; Healy, E. F.; Stewart, J. J. *J. Am. Chem. Soc.* **1985**, *107*, 3902. (b) Dewar, M. J. S. *A Semiempirical Life. In Profiles, Pathways, and Dreams. Autobiographies of Eminent Chemists*; Seeman, J. I., Ed.; American Chemical Society: Washington, DC, 1992.

(27) Wheatley, P. J. *Acta Crystallogr.* **1957**, *10*, 182.
(28) *CRC Handbook of Chemistry and Physics*, 69th ed.; CRC Press: Boca Raton, FL, 1988; p F-165.

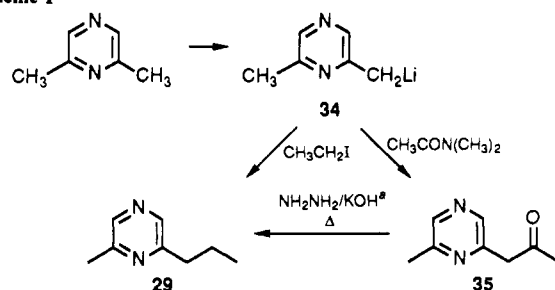
(29) Schomaker, V.; Pauling, L. *J. Am. Chem. Soc.* **1939**, *61*, 1769.

(30) Tamao, K.; Kodama, S.; Nakajima, I.; Kumada, M.; Minato, A.; Suzuki, K. *Tetrahedron* **1982**, *22*, 3347.

(31) For a recent report on the preparation of deuterated methylpyridines and references therein, see: Lautie, M.-F.; Leygue, N. *J. Labelled Compd. Radiopharm.* **1991**, *29*, 813.

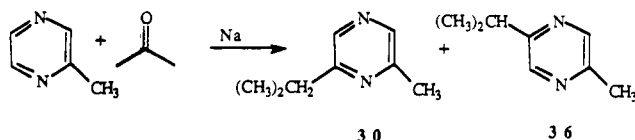
(32) Ohta, A.; Ohta, M.; Igarashi, Y.; Saeki, K.; Yuasa, K.; Mori, T. *Heterocycles* **1987**, *26*, 2449.

Scheme I

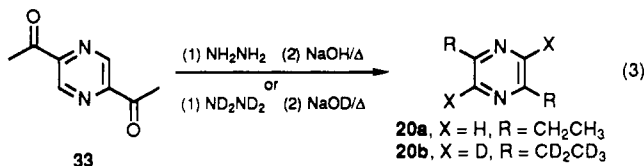


^a 2-Methyl-6-isopropylpyrazine (30) is also formed in this reaction (see Scheme II).

Scheme II



Wolff–Kishner reduction of 2,5-diacetylpyrazine^{33,34} (33) proceeds without incident to the desired 2,5-diethylpyrazine (20a) as displayed in eq 3. Analogously, 2,5-diethylpyrazine-*d*₁₂ (20b) was prepared from 15



using hydrazine, NaOD, diethylene glycol, and D_2O employing toluene as the azeotropic solvent. The reaction is performed in one pot but in multiple steps: the first series served to exchange the solvent and the hydrazine protons; base was then added to effect the exchange of the methyl protons, followed by disproportionation of the fully deuterated hydrazone in the presence of the resulting deuterated solvents after the exchanges with D_2O were complete, and the toluene had been distilled off. Interestingly, the reaction conditions caused exchange of the ring protons as well.

2-Methyl-6-propylpyrazine (29) can be prepared by two methods (Scheme I), both of which involve tedious workups. 6-Methyl-2-pyrazinylmethylithium (34) reacts with iodoethane to give a complex mixture from which 29 is isolated. Alternatively, 34 is allowed to react with *N,N*-dimethylacetamide to afford, upon workup, easily purifiable 2-methyl-6-(2-oxopropyl)pyrazine (35). The Wolff–Kishner reduction of 35 could provide 29 directly; however, this strategy is complicated by the accompaniment of an unanticipated rearrangement, described in full detail elsewhere,³⁵ in which 29 is formed along with 2-methyl-6-isopropylpyrazine (30) (see Scheme II). Centrifugal chromatography can be employed to isolate sufficient quantities of 29 for our spectroscopic studies.

2-Methyl-6-isopropylpyrazine (30) can be prepared by a literature procedure³⁶ involving the reaction of acetone with methylpyrazine and sodium metal in absolute diethyl ether as shown in Scheme II. Elaborate workup is needed to remove unreacted starting material, acetone self-condensation products including mesityl oxide, and the isomeric 2-methyl-5-isopropylpyrazine (36) which is also formed. Because pyrazine 30 is also isolated from the Wolff–Kishner reduction of 35 (cf. Scheme I) as one of the byproducts, confirmation of the structural assignments made for 29, 30, and 36 is thereby provided.

C. Synthesis of Substituted Pyridines and Pyrazines. Experimental Details. Propylpyrazine (6). A solution of chloropyrazine (15.0 g, 0.131 mol) and 1,3-bis(diphenylphosphino)propanedichloronickel(II) [Dppp-NiCl₂, obtained from Strem Chemicals] (517 mg, 0.93 mmol) in diethyl

ether (300 mL) was treated dropwise with 2 M propylmagnesium chloride (78.5 mL, 0.157 mol) with cooling (0 °C). The resulting yellow solution was heated at reflux for 18 h. Ice was added and the organic layer was separated and extracted with 6 N HCl (36 mL). The acidic phase was washed with ether, basified (50% KOH) and extracted with ether. The ethereal phases were combined and dried (Na_2SO_4), and the solvent was removed to yield propylpyrazine (6) which was isolated by distillation: bp 60 °C (aspirator vacuum); 8.81 g (55%); ¹H NMR (CDCl_3) δ 0.99 (3 H, t, $J = 7.4$ Hz), 1.79 (2 H, sextet, $J = 7.5$ Hz), 2.80 (2 H, t, $J = 7.6$ Hz), 8.40 (1 H, d, $J = 2.5$ Hz), 8.50 (2 H, m); ¹³C NMR (CDCl_3 at 77.19) δ 13.76 (C-3'), 22.68 (C-2'), 37.46 (C-1'), 142.11, 144.04, 144.64, 157.77 (C-2).

Propyl-*d*₇-pyrazine (21). This preparation was carried out in the same manner as 6 using chloropyrazine (4.40 g, 38.5 mmol), Dppp-NiCl₂ (250 mg, 0.46 mmol), ether (100 mL), and propyl-*d*₇-magnesium bromide [prepared from propyl-*d*₇ bromide (5.0 g, 38.5 mmol) and magnesium turnings (1.01 g, 46.2 mmol) in ether (9 mL)]. Propyl-*d*₇-pyrazine (21) was isolated by distillation: bp 60 °C (aspirator vacuum); 2.45 g (49.3%); ¹H NMR (CDCl_3) δ 8.40 (1 H, d, $J = 2.8$ Hz), 8.47 (1 H, d, $J = 1.6$ Hz), 8.50 (1 H, t, $J = 2$ Hz), minute peaks at δ 0.92, 1.73, and 2.76 marked traces of the protium isotope on the propyl group; ¹³C NMR (CDCl_3 at 77.37) δ 12.60 (septet, $J = 19.1$ Hz), 21.52 (quintet, $J = 19.2$ Hz), 36.47 (quintet, $J = 19.4$ Hz), 142.13, 144.05, 144.63, 157.76 (C-2).

Methyl-*d*₃-pyrazine (11). This preparation was carried out in the same manner as described for 6 using chloropyrazine (9.54 g, 83.3 mmol), Dppp-NiCl₂ (330 mg, 0.61 mmol), methyl-*d*₃-magnesium iodide (1 M, 100 mL, 0.1 mol), and ether (200 mL). Methyl-*d*₃-pyrazine (11) was isolated by distillation: bp < 20 °C (0.1 mm); 880 mg (11%); ¹H NMR (CDCl_3) δ 2.28 (trace of methyl-H), 8.39 (1 H, d, $J = 2$ Hz), 8.47 (2 H, m). This last may also be interpreted as: δ 8.47 (1 H, d, $J = 2$ Hz), 8.48 (1 H, s). ¹³C NMR (CDCl_3 at 77.09) δ 20.84 (1 C, septet, $J = 19.6$ Hz), 141.89, 143.90, 144.86, 154.06 (C-2).

2,5-Diethylpyrazine (20a). 2,5-Diacetylpyrazine (mp 159–160 °C, prepared by the free-radical acetylation of acetylpyrazine^{33,34}) (5.0 g, 30.5 mmol) and anhydrous hydrazine (5.9 mL, 176 mmol) were refluxed in ethanol (150 mL) for 1 h. The mixture was cooled to 0 °C and the product bishydrazone recovered by filtration; the solids were rinsed with ethanol and ether. The dried product weighed 5.63 g (96%), mp 213–216 °C. This bishydrazone (6.56 g, 34.1 mmol), KOH (2.92 g, 85%), and diethylene glycol (35 mL) were stirred and heated to 155 °C (oil bath, 1 h). Nitrogen gas evolved steadily, and a dark red solution resulted. The mixture was quenched with ice/water and extracted (3 × 100 mL) with dichloromethane. The combined extracts were dried and concentrated in vacuo. The resulting clear light brown oil (4.71 g) was distilled through a 5 cm Vigreux column to afford 4.21 g (90.6%) of 20a: bp 35 °C (0.3 mmHg); ¹H NMR (CDCl_3) δ 1.33 (6 H, t, $J = 7.6$ Hz), 2.82 (4 H, q, $J = 7.6$ Hz), 8.38 (2 H, s); ¹³C NMR (CDCl_3) δ 13.26 (2 C: CH_3CH_2), 27.85 (2 C: CH_3CH_2), 142.35 (C-3,6), 155.08 (C-2,5).

2,6-Diethylpyrazine (19a). 2,6-Dichloropyrazine (5.01 g, technical grade, Aldrich) was dissolved in toluene and filtered through a cotton plug to remove minor sediment and traces of water droplets. The filtrate was diluted with toluene to 150 mL, and 1,3-bis(diphenylphosphino)propanedichloronickel(II) (ca. 60 mg) added. The mixture was stirred magnetically at room temperature under N_2 as diethylzinc (1.1 M in toluene, Aldrich, 74 mL) was added slowly by syringe, (20 min). The reaction was noticeably exothermic. The mixture was stirred for 2.5 h; a sample was quenched with NH_4OH and examined by TLC [5% acetone (v/v)—hexane, silica gel]; a single mobile spot was revealed. The mixture was stirred as 1:1 (v/v) concentrated NH_4OH – H_2O (100 mL) was added cautiously (evolution of ethane). The reaction mixture was filtered, and the reaction vessel and solids were rinsed with hexane. The organic phase was isolated from the filtrate, extracted with a solution of H_2SO_4 (9.9 mL) in H_2O (75 mL), then with a solution of concentrated HCl (11.5 mL) in H_2O (70 mL). The two aqueous phases were separately basified by K_2CO_3 to pH 11; each was extracted with hexane (100 mL). The combined extracts were concentrated in vacuo to give an oil (3.76 g), which was Kugelrohr distilled to afford a yield of 3.38 g (74%, nominal). The yield obtained is easily diminished by the volatility of the product and its incomplete extraction into strong acids; the actual conversion of the dichloropyrazine to product is nearly quantitative, based on the TLC evidence: ¹H NMR (CDCl_3) δ 1.33 (6 H, t, $J = 7.5$ Hz), 2.82 (4 H, q, $J = 7.5$ Hz), 8.28 (2 H); ¹³C NMR (CDCl_3 at 76.94) δ 13.69 (2 C: CH_3CH_2), 28.70 (2 C: CH_3CH_2), 140.72 (3, 5), 157.44 (2, 6).

2-Methyl-6-propylpyrazine (29). 2,6-Dimethylpyrazine (10.88 g, 0.1006 mol) and diethyl ether (215 g) were cooled in ice under N_2 . Diisopropylamine (10 mL, 0.071 mol) was added, followed, dropwise by *n*-butyllithium (43 mL, 2.5 M in hexanes, 0.1075 mol), while the mixture was stirred magnetically. After 5 min of further stirring, iodoethane (9 mL, 0.11 mol) was added, and the mixture was stirred overnight at room

(33) Houminer, Y.; Southwick, E. W.; Williams, D. L. *J. Org. Chem.* **1989**, *54*, 640.

(34) Caronna, T.; Fronza, G.; Minisci, F.; Porta, O. *J. Chem. Soc., Perkin Trans. 2* **1972**, 2035.

(35) Paine, J. B., III *J. Heterocycl. Chem.* **1991**, *28*, 1463.

(36) Bramwell, A. F.; Payne, L. S.; Riezebos, G.; Ward, P.; Wells, R. D. *J. Chem. Soc. C* **1971**, 1627.

temperature. Water (50 mL) was then added. On being allowed to stand the ether evaporated. The product was extracted with hexane, and the solvent was removed in vacuo to give a crude oil (10.22 g). Upon Kugelrohr distillation, 9.17 g of volatile material was isolated. This was subjected to column chromatography in two lots [Silica Gel 60, 10% (v/v) acetone in *n*-hexane]. The fractions of appropriate polarity (corresponding to the middle spot of the three principal spots observed by TLC) were combined, and the contained product subjected to spinning-band distillation (water aspirator vacuum). The resulting **29** (the most volatile remaining component) was 100% pure by GC: $^1\text{H NMR}$ (CDCl_3) δ 0.99 (3 H, t, $J = 7.4$ Hz), 1.76 (2 H, sextet, $J = 7.5$ Hz), 2.54 (3 H, s), 2.75 (2 H, t, $J = 7.7$ Hz), 8.25 (1 H, s), 8.28 (1 H, s); $^{13}\text{C NMR}$ (CDCl_3 at 76.92) δ 13.79 ($\text{CH}_2\text{CH}_2\text{CH}_3$), 21.54 (2- CH_3), 22.96 ($\text{CH}_2\text{-CH}_2\text{CH}_3$), 37.48 ($\text{CH}_2\text{CH}_2\text{CH}_3$), 140.96 (5), 141.48 (3), 152.60 (6), 156.21 (2).

2-Methyl-6-(1-methylethyl)pyrazine (30).³⁶ Sodium metal (25.79 g, 1.12 g-atoms) was melted under toluene in an atmosphere of N_2 and dispersed with the addition of oleic acid (1–2 mL). The resulting sodium sand was allowed to cool and solidify undisturbed. It was then rinsed and decanted first with hexane, subsequently with three aliquots of absolute diethyl ether. Absolute diethyl ether (400 mL) was added and the suspension stirred magnetically under a reflux condenser, as a mixture of methylpyrazine (53.45 g, 0.568 mol) and acetone (36.97 g, 48 mL, 0.637 mol) was added over 37 min. Stirring was continued under N_2 overnight. The reaction mixture was decanted from most of the unreacted sodium metal and treated under N_2 with methanol (ca. 50 mL) to help destroy remaining traces of Na metal. Water (200 mL) was then added carefully, also under N_2 ; the last of the Na metal quickly reacted. The resulting organic phase was isolated. Ether was removed at 30 °C (rotary evaporator), and much of the unreacted methylpyrazine was removed at 70 °C. The product was distilled over on the rotary evaporator at 100 °C; the last traces were fished out of the residue by Kugelrohr distillation. Column chromatography of the combined product concentrates [Silica Gel 60, 175 g, 10% (v/v) acetone/hexane] served to remove remaining methylpyrazine and other more polar materials. The appropriate fractions (totalling 9.24 g) were combined with similar material from a previous run (2.43 g) and subjected to spinning-band distillation (water-aspirator vacuum). Product **30** (8.72 g) was obtained in ca. 90% purity, contaminated principally by mesityl oxide resulting from acetone self-condensation. Less pure fractions were distilled separately to afford further concentrate (2.02 g). The final purification of 2-methyl-6-isopropylpyrazine (**30**) from the 2,5-isomer **36** was effected by HPLC on silica gel, using 20% ethyl acetate (v/v) in hexane. The desired isomer eluted first. The appropriate fractions were combined and stripped on a rotary evaporator, and the residue was Kugelrohr distilled

(bp < 39 °C (0.28 Torr)): $^1\text{H NMR}$ (CDCl_3) δ 1.33 (6 H, d, $J = 7$ Hz), 2.54 (3 H, s), 3.07 (1 H, septet, $J = 7$ Hz), 8.28 (1 H, s), 8.29 (1 H, s); $^{13}\text{C NMR}$ (CDCl_3 at 77.11) δ 21.61 (2- CH_3), 22.24 (2C: Me_2CH), 34.14 (Me_2CH), 139.60 (5), 141.85 (3), 152.70 (2), 161.25 (6). This material had the same GC retention time as the byproduct from the Wolff-Kishner reduction of 1-(6-methyl-2-pyrazinyl)-2-propanone (**35**), confirming the relative isomeric structure.³⁵

2-Ethyl-*d*₅-pyridine (13). Magnesium turnings (2.31 g, 95 mg-atoms) were warmed with iodine (ca. 1 mg) under N_2 in a 50 mL three-necked round bottom flask until purple fumes were visible. The apparatus was then cooled under N_2 to room temperature, and anhydrous diethyl ether (20 mL) added. Ethyl-*d*₅ bromide (10 g, 87.7 mmol) was placed in an addition funnel atop the condenser, and ca. 1 g was added to start the reaction. The reaction mixture was warmed gently, and the reaction, once initiated, was maintained by the gradual addition of the remaining halide. After the addition had been completed, the dark cloudy mixture was refluxed an additional 15 min. The resulting Grignard solution was added by syringe to a cooled (–5 °C) solution of 2-bromopyridine (11.55 g, 73.0 mmol) in anhydrous diethyl ether (80 mL) containing Dppp-NiCl_2 (0.425 g, 0.78 mmol). An exothermic reaction occurred, and the temperature was brought to and maintained at 30 °C with external cooling. The mixture was stirred at room temperature for 2.5 h, then treated with 5% HCl (75 mL), to give a pH of 1. The aqueous phase was rinsed 3× with ether (discarded), then basified with K_2CO_3 (7.5 g), then 50% KOH. The product was extracted into ether (3×), dried (Na_2SO_4), and concentrated in vacuo. The residue was distilled through a 5 cm Vigreux column, bp 57 °C (32 Torr), to give 6.60 g (80.6%) of **13**: $^1\text{H NMR}$ (CDCl_3) δ 7.07 (1 H, m), 7.14 (1 H, m), 7.57 (1 H, m), 8.52 (1 H, m). Traces of ethyl protons were noted at ca. 1.26 and 2.78. $^{13}\text{C NMR}$ (CDCl_3 at 77.23) δ 12.90 (septet, $J = 19.4$ Hz, CD_3), 30.49 (quintet, $J = 19.4$ Hz, CD_2), 120.87, 122.03, 136.32 (C-4), 149.15 (C-6), 163.45 (C-2). The picrate was prepared in ethanol, mp 107–108 °C.

Acknowledgment. We thank R. L. Bassfield, J. Naworal, and N. Jensen for assistance in obtaining spectroscopic data and Professor A. Streitwieser, Jr. and the reviewers for helpful comments.

Registry No. **2**, 109-08-0; **3**, 109-06-8; **4**, 13925-00-3; **5**, 100-71-0; **6**, 18138-03-9; **7**, 622-39-9; **8**, 29460-90-0; **9**, 644-98-4; **11**, 139607-04-8; **13**, 139607-05-9; **19a**, 13067-27-1; **19b**, 139607-06-0; **20a**, 13238-84-1; **20b**, 139607-07-1; **21**, 139607-08-2; **29**, 29444-46-0; **30**, 24541-74-0; **33**, 39248-49-2; **33** dihydrazone, 139607-09-3; D_2 , 7782-39-0; chloropyrazine, 14508-49-7; 2,6-dichloropyrazine, 4774-14-5; 2,6-dimethylpyrazine, 108-50-9.